RAPID COMMUNICATIONS

PHYSICAL REVIEW E VOLUME 49, NUMBER 5 MAY 1994

Transition from quasiperiodicity to chaos of a soliton oscillator

M. Cirillo,* A. R. Bishop, N. Grønbech-Jensen, and P. S. Lomdahl

Theoretical Division and Center for Nonlinear Studies, Los Alamos National Laboratory, Los Alamos, New Mexico 87545

(Received 31 January 1994)

We study the properties of the quasiperiodic attractors of the driven and damped sine-Gordon system close to the onset of chaotic dynamics. Our system is a perturbed sine-Gordon equation with ac and dc forcing terms over a finite-size spatial interval. In this system the quasiperiodic trajectories are generated by the incommensurability of the soliton oscillation and external drive frequencies. For increasing values of the ac drive amplitude the attractors of the system, displayed in a spatially averaged Poincaré section, present the characteristic folding and mixing properties of the transition to chaos through quasiperiodicity. In the parameter plane that we scan, the basic features of the transition are not dependent upon the particular ac drive amplitude and frequency causing the transition. Analysis of the singularity spectrum $f(\alpha)$ of several attractors at the chaotic threshold exhibits general features of the transition.

PACS number(s): 03.40.Kf, 74.50.+r, 74.60.Ge

The study of chaotic states of the driven and damped sine-Gordon (SG) equation began a decade ago and a number of works were dedicated to the onset of chaos under particular dynamical conditions and choices of forcing terms [1–5]. An intriguing aspect of the transition to chaos in the SG system is the existence of an obvious competition between the background chaotic tendencies, due to the well known chaotic dynamics of the driven pendulum [6], and the coherent spatial patterns composed of soliton oscillations. Therefore the study of the transition to chaos in this system can yield information for a class of systems in which spatiotemporal competitions exist [7].

The first work dealing with the spatiotemporal chaos in the sine-Gordon system was by Bishop *et al.* [1]. These authors considered a driven sine-Gordon equation including a uniform ac forcing term over a spatial interval on which they imposed periodic boundary conditions. Due to the absence of the dc forcing terms the spatiotemporal competition in this case was limited to breather and plasma modes and background oscillations. Somewhat similar phenomena were later reported by Guerrero and Octavio [4].

The interest for potential practical applications of collective excitations of soliton oscillators based on long Josephson junction devices moved much interest to the spatial modes of the ac driven sine-Gordon equation over a finite spatial interval with various boundary conditions. Extensive numerical simulations [3,5,8], analytical approaches [9,10], and experiments [11] have been devoted to the long Josephson junctions operated in the soliton oscillation regime. Even when operated in this regime, the chaotic patterns generated by the strong tendency of the solitons to maintain their oscillatory motion and the chaotic background were evident [5]. The oscillatory motion of solitons in the sine-Gordon system can be obtained for adequate choice of dissipation and forcing terms [12,13].

In this paper we report on the transition from the quasiperiodicity, generated by the incommensurability between the soliton oscillation and external ac drive frequencies, and more complicated dynamical states giving rise to folding and mixing of the attractors in the Poincaré sections. We study the singularity spectrum of the attractors close to the onset of these complicated dynamical states and analyze their properties through their $f(\alpha)$ functions [14]. This study is performed for single soliton oscillations, fixing the dc forcing term but varying the ac drive amplitude and frequency.

The system we investigate is governed by the equation

$$\phi_{tt} - \phi_{xx} + \sin\phi + \gamma\phi_t = \rho_0 + \rho_1 \sin(\omega t) \ , \qquad (1)$$

with the boundary conditions

$$\phi_x(0,t) = \phi_x(l,t) = 0 \ . \qquad (2)$$

In Eqs. (1) and (2) time and space are normalized to standard parameters [1–5]. In terms of Josephson junctions phenomenology the above equations model a long Josephson junction (LJJ) having uniformly distributed dc and rf currents over the extended spatial dimension, and open circuit boundary conditions [5]. An extensive study of the solutions of our system over the plane of the parameters ρ_1 and ω was performed by one of us for $l = 4.8\bar{3}$ and $\gamma = 0.252$ [5]. The region that was scanned was the area close to the lowest threshold for the onset of chaotic dynamics and, therefore, close to $\omega = 1$ [6]. As a specified context for our investigations we have used the same parameter values reported in Fig. 1 of Ref. [5]. We note that in the latter work no attempt was made to describe in detail the transition to chaos of the system. For the parameter choice reported above, the frequency of the soliton oscillations (the inverse of the time taken for the single soliton to complete one back and forth journey along the spatial interval) is 0.5145. Twice this frequency (1.029) is termed the "proper" oscillation frequency in Ref. [5].

*Permanent address: Dipartimento di Fisica, Università di Roma "Tor Vergata," I-00133 Roma, Italy.

Our investigation of the chaotic transition proceeded as follows. We fixed a point in the (ω, ρ_1) plane below the threshold for the onset of the chaos and then, always keeping $\rho_0 = 0.5$ (this was the value of the driving force used in Ref. [5]), for a constant value of the drive frequency ω we gradually increased the value of ρ_1. The results of the numerical integration of the system described by Eqs. (1) and (2) were then displayed in terms of (a) a Poincaré section averaged over the entire spatial interval and (b) the Fourier transform of the corresponding output wave forms: these were our main diagnostic tools for analyzing the response of the system.

A typical result of our numerical experiments is shown in Fig. 1. In Fig. 1(a), from the top to the bottom, the four curves have been obtained respectively for ρ_1=0.0, 0.25, 0.45, 0.558; fixing $\rho_0 = 0.5$ and $\omega = 0.91$. We can clearly see that for the lower amplitudes of the ac drive the quasiperiodic trajectory is very smooth with a maximum and a minimum situated respectively around 0 and $\pi/2$. With further increase of the value of ρ_1 up to 0.45 (third curve from the top) the smooth quasiperiodic trajectories start bending, showing typical features

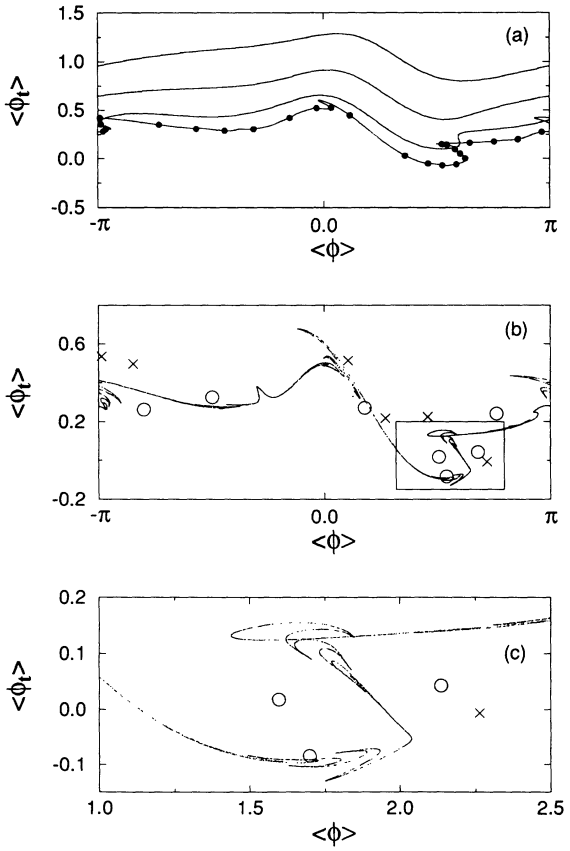

FIG. 1. (a) Quasiperiodic trajectories obtained for increasing values of the ac drive amplitude, fixing $\omega = 0.91$. The lowest trajectory is the *critical* one obtained for $\rho_1 = 0.558$. Increasing ρ_1 to 0.559 the system locks on the period 25 subharmonic. (b) Fractal attractor obtained for $\rho_1 = 0.582$. The circles and the crosses indicate periodic solutions generated by a small dc forcing term perturbation. An amplification of the area indicated by the square is shown in (c). Axes are in normalized units.

observed for other quasiperiodic attractors close to the onset of chaos [15]. However, in our case the bending of the curves does not evolve directly into more complicated attractors as often happens with other systems [4,15]. In fact, the value $\rho_1 = 0.558$ (fourth curve from the top) represents a *critical* threshold after which the system locks on the 25th subharmonic, as indicated by the full dots in Fig. 1(a). The period 25 persists from $\rho_1 = 0.559$ up to $\rho_1 = 0.564$, after which the system evolves into more complicated dynamical states. This is a general feature that we have found in our numerical experiments. The points of the period 25 solution are dispersed around the *critical* quasiperiodicity attractor, which is the one obtained for $\rho_1 = 0.558$.

In Fig. 1(b) we show the attractor obtained upon increasing the ac drive amplitude to 0.582: a magnification of the area indicated by the square in Fig. 1(b), reported in Fig. 1(c), clearly shows its bending and folding properties. An interesting feature of our simulations is the fact that, given a "chaotic" attractor obtained by fixing the ac amplitude and frequency, a small perturbation of the dc bias current can trigger the system toward a periodic orbit. An example of this phenomenon for the attractor that we are considering is also shown in Figs. 1(b) and 1(c). The empty circles in Figs. 1(b) and 1(c) represent the period 7 solution that we obtain for $\rho_0 = 0.495$, while the crosses correspond to the period 6 solution that we obtain for $\rho_0 = 0.505$. Thus these periodic solitons represent the effect of a dc-bias perturbation around $\rho_1 = 0.582$ and $\omega = 0.91$. This kind of behavior is closely reminiscent of the results obtained for other dynamical systems in which chaos can be controlled by small perturbations [16]. We note that this "stabilizing" effect of our chaotic attractor only operates for very small perturbations: Increasing the dc-bias force even a factor 0.1 above or below 0.5 the system exhibits completely different attractors and chaotic states.

We note that the locking on high degree subharmonics could be an indication of overlapping of Arnold tongues [17], especially if we note that the periodicity of the locking depends on the value of the applied frequency. A common feature of our subharmonic locking with the overlapping of Arnold tongues is the fact that this latter phenomenon determines the threshold for the transition to chaos via quasiperiodicity in a number of systems [15,17]. In our system, we have always found that the transition to chaos was anticipated by the locking on high degree subharmonics. Unfortunately, a careful frequency scan to verify the possible existence of these tongues requires, in the present case, a prohibitive amount of computing.

We have reproduced, however, the same kind of phenomenology observed for the drive frequency $\omega = 0.91$ for several other values of the frequency and in some cases locking up to the 40th subharmonic of the drive frequency was found. We note that the generation of high degree subharmonics is not new for the Josephson junctions related dynamics [6] of the driven pendulum; however, the scenario that we are describing, to our knowledge, has not been reported previously. The value of the ac amplitude for which we find the jump from quasiperiodic trajectories to chaos depends on the value of the drive

frequency, but its value always lies below the border for the onset of chaos reported in Fig. 1 of Ref. [5].

A more experiment oriented sequence of the phenomena that we have described above is shown in Fig. 2. In this figure we report the power spectrum of the time series corresponding to $\rho_1 = 0.25$ (a), 0.55 (b), 0.56 (c), and 0.582 (d) (the value of the drive frequency is 0.91 for all cases). The spectra of Fig. 2 give another clear representation of the dynamics of our driven, damped sine-Gordon system. We see that, when the ac-drive amplitude is far below the critical value for switching to the subharmonic behavior [Fig. 2(a)], there exist some bunched subharmonic lines at multiples of the seventh subharmonic but, even if the background noise is low, the spectrum is somewhat irregular. This kind of spectrum reminds us of the ones reported previously for the driven long Josephson junction [9,11]. In Fig. 2(b), very close to the critical amplitude, we find a spectrum very rich in harmonic content with an increased background noise level, but still somewhat regular in the spacing of the components. In Fig. 2(c) we see in the frequency domain the 25th subharmonic locking while in Fig. 2(d) we see a typical chaotic spectrum with random frequency components and increased background noise level.

Since we found that the general properties of the transition to chaos of our system were independent of the particular point on the amplitude-frequency plane that we were investigating, we tried to characterize all our attractors in a more quantitative fashion. One possibility is to measure their singularity spectrum, $f(\alpha)$ [14]. We have measured this spectrum with two different methods which gave similar results. The first method uses a Legendre transformation to smooth the experimental data [14]; the second method is based on the Shannon [18] definition of entropy and was proposed by Chhabra and Jensen [19]. This latter method has also been successfully employed by other authors for the analysis of experimental data [20]. The results that we show below are all based on this second method, which we found very versatile for the analysis of our data. We will report on a full comparison of the two methods, applied to our problem, in a future paper.

The details of the method that we employ were well described in Ref. [19]. The basic procedure consists of dividing the area of the attractor into boxes whose size $L = 1/N$ (in our case we found that the most reasonable value of N was of the order of 60). Counting the number of points of the attractor falling in the ith box, one can evaluate the probability P_i associated with it; then we construct the family of normalized measures from the probabilities defined as $\mu_i(q, L) = [P_i(L)]^q / \sum_j [P_j(L)]^q$. After evaluating P_i and $\mu_i(q, L)$, the calculation of the measure $f(\alpha)$ and the singularity strength α are straightforward [19]. We performed this procedure for a box-size sequence like [1,2,3,..., n] and sequences like [$2^1, 2^2, 2^3, \ldots, 2^n$] and these two processes gave results consistent within the experimental error. In Fig. 3 we show typical results of the determination of α and $f(\alpha)$. We can see that our plots have the same features as usually described [19,20]: for positive values of q (corresponding to the leftmost portion of the curves) the linear regressions [19] produce a small error while the negative q values give rise to a wide

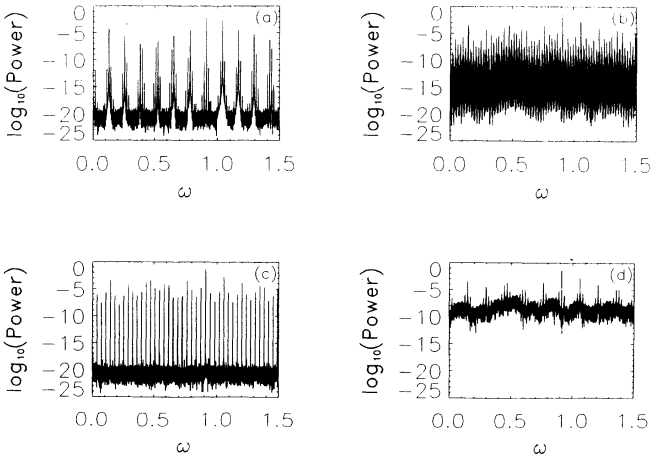

FIG. 2. Power spectra corresponding to the sequence $\rho_1 = 0.25$ (a); 0.55 (b); 0.56 (c); 0.582 (d). The passage from (b) to (c) to (d) clearly indicates a discontinuity in the dynamical response of the system. In between the two noisy spectra (b) and (d) we have a stable subharmonic locking. Axes are in normalized units.

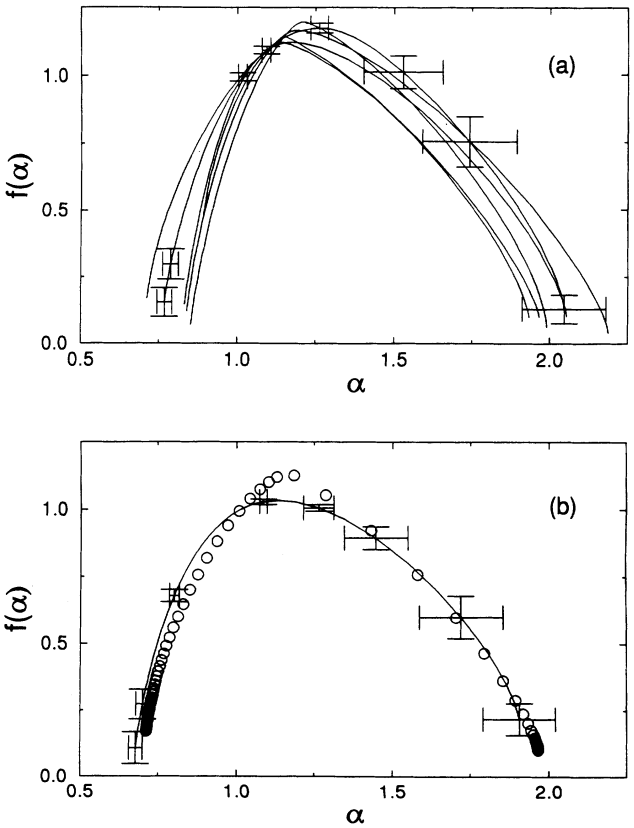

FIG. 3. (a) The $f(\alpha)$ curves obtained for some of the critical attractors that we have obtained. We show here, for figure clarity, only the error bars of one curve. (b) Comparison of the orbit obtained for $\rho_1 = 0.2712$, $\omega = 0.4$ (circles) with the critical golden mean attractor of the circle map (continuous curve, with error bars). Axes are in normalized units.

spread of the data generating a larger error.

In Fig. 3(a) we report the $f(\alpha)$ function for several critical attractors that we have observed. Those attractors are the ones obtained for different frequencies when the value of the ac drive is just below the point where the system locks on subharmonics. We can see in this figure that all the curves are consistent within the numerical uncertainty (we only depict the error bar for one of the curves). This phenomenon confirms our impression that the transitions to chaos may have properties which are not dependent upon the particular frequency at the transition. The other interesting feature of our threshold attractors is the fact that their singularity spectrum is very close to that of the circle map at the golden mean transition [14,17]. The similarities of our attractors with those obtained from the orbit of the circle map are shown with greater emphasis in Fig. 3(b), where we superimpose the $f(\alpha)$ curve for the critical orbit of the circle map (full line) and one of our critical attractors (circles) obtained for a drive frequency $\omega = 0.4$ and a drive amplitude $\rho_1 = 0.2712$.

We note that the drive frequency of Fig. 3(b) has *not* been chosen in order to have a normalized frequency (soliton oscillation frequency divided by drive frequency) of th order of the golden mean. This ratio for the curve of Fig. 3(d) is 1.286 larger than unity, which could be an indication that the basic dynamic mechanism is somewhat different. Nevertheless, the similarity of our singularity spectra with that of the circle map is very striking, especially noting that in the negative q region all the curves of Fig. 3(a) fall within the error bar obtained for the circle map.

In conclusion, we have described a scenario for the transition to chaos from quasiperiodicity of a soliton oscillator driven by an ac signal whose frequency is below the plasma frequency of the sine-Gordon system. We have focused on features of the scenario that are not dependent on the particular frequency of the ac drive chosen for observing the transition. An analysis of the attractors close to the threshold for onset of the chaotic states, performed in terms of singularity spectra, reveals notable commonalities and very close similarities to the transition to chaos of the circle map at the golden mean frequency. We note that some of the features that we have reported could have interesting practical counterparts if we consider that a fluxon oscillator [5,11,13], which is the Josephson junction counterpart of our system of Eqs. (1) and (2), can oscillate in the microwave and millimeter-wave range of the electromagnetic spectrum. Our simulations show that, when the oscillator is driven close to its plasma frequency [12], it may have noticeable down converting capabilities over significant frequencies intervals.

We acknowledge fruitful discussions with Paola Cocciolo, Mogens H. Jensen, and Angel Sánchez. This work has been partially supported by the Progetto Finalizzato "Tecnologie Superconduttive e Criogeniche" (Sucrytec) of the CNR (Italy) and by the U.S. Department of Energy.

[1] A. R. Bishop, K. Fesser, P. S. Lomdahl, W. C. Kerr, M. B. Williams, and S. E. Trullinger, Phys. Rev. Lett. **50**, 1095 (1983).
[2] O. H. Olsen and M. R. Samuelsen, Appl. Phys. Lett. **47**, 1007 (1985).
[3] N. F. Pedersen and A. Davidson, Phys. Rev. B **41**, 178 (1990).
[4] L. E. Guerrero and M. Octavio, Phys. Rev. A **37**, 3641 (1988).
[5] M. Cirillo, J. Appl. Phys. **60**, 338 (1986).
[6] R. L. Kautz and R. Monaco, J. Appl. Phys. **57**, 875 (1985).
[7] *Spatio-Temporal Coherence and Chaos in Physical Systems*, edited by A. R. Bishop, G. Grüner, and B. Nicolaenko (North-Holland, Amsterdam, 1986).
[8] G. Rotoli, G. Costabile, and R. D. Parmentier, Phys. Rev. B **41**, 1958 (1990).
[9] M. Salerno, M. R. Samuelsen, G. Filatrella, S. Pagano, and R. D. Parmentier, Phys. Rev. B **41**, 6641 (1990).
[10] Niels Grønbech-Jensen, Phys. Lett. A **169**, 31 (1992).
[11] R. Monaco, S. Pagano, and G. Costabile, Phys. Lett. A **131**, 122 (1988).
[12] A. Barone and G. Paternò, *Physics and Applications of the Josephson Effect* (Wiley, New York, 1982).
[13] D. W. McLaughlin and A. C. Scott, Phys, Rev. A **18**, 1672 (1978).
[14] T. C. Halsey, M. H. Jensen, L. P. Kadanoff, I. Procaccia, and B. Shraiman, Phys. Rev. A **33**, 1141 (1986).
[15] E. G. Gwinn and R. M. Westervelt, Phys. Rev. Lett. **59**, 157 (1987).
[16] T. Shinbrot, C. Grebogi, E. Ott, and J. A. Yorke, Nature (London) **363**, 411 (1993).
[17] M. H. Jensen, P. Bak, and T. Bohr, Phys. Rev. A **30**, 1960 (1984).
[18] C. Shannon, Bell. Syst. Tech. J. **27**, 379 (1948).
[19] A. Chhabra and R. V. Jensen, Phys. Rev. Lett. **62**, 1327 (1989).
[20] A. Sánchez, F. Guinea, L. M. Sander, V. Hakim, and E. Louis, Phys. Rev. E **48**, 1296 (1993); A. Sánchez, R. Serna, F. Catalina, and C. N. Afonso, Phys. Rev. B **46**, 487 (1992).